

# COVID-19 Disease Prediction Using Weighted Ensemble Transfer Learning

Pradeep Kumar Roy<sup>1</sup>, Ashish Singh<sup>2</sup> \*

<sup>1</sup> Department of Computer Science & Engineering, Indian Institute of Information Technology, Surat Gujarat-394190 (India)

<sup>2</sup> School of Computer Engineering, KIIT Deemed to be University, Bhubaneswar-751024, Odisha (India)

Received 28 January 2022 | Accepted 25 January 2023 | Early Access 7 February 2023



## ABSTRACT

Health experts use advanced technological equipment to find complex diseases and diagnose them. Medical imaging nowadays is popular for detecting abnormalities in human bodies. This research discusses using the Internet of Medical Things in the COVID-19 crisis perspective. COVID-19 disease created an unforgettable remark on human memory. It is something like never happened before, and people do not expect it in the future. Medical experts are continuously working on getting a solution for this deadly disease. This pandemic warns the healthcare system to find an alternative solution to monitor the infected person remotely. Internet of Medical Things can be helpful in a pandemic scenario. This paper suggested a ensemble transfer learning framework predict COVID-19 infection. The model used the weighted transfer learning concept and predicted the COVID- 19 infected people with an F1-score of 0.997 for the best case on the test dataset.

## KEYWORDS

Convolutional Neural Network, COVID-19, Deep Learning, Ensemble Learning, Healthcare, Transfer Learning.

DOI: 10.9781/ijimai.2023.02.006

## I. INTRODUCTION

WITH the advancement of computer science technology, healthcare devices are also smart and capable of recording the patient's health information like Blood pressure, Body Temperature, and others with the help of different kinds of sensors. The captured information is further passed to Health experts using connected devices [1], [2], [3]. One Internet of Medical Things (IoMT) scenario is shown in Fig. 1. Different components involved in setting up the IoMT environment are shown, along with a tentative flow of healthcare information between patients and health experts. In the IoMT environment, mainly two components are present- (i) different kinds of sensors and (ii) connective devices. The sensors are used to collect the patient's health information, and networking devices are used to pass the collected information to the concerned medical expert. With IoMT environment, it is possible that multiple patients are being monitored by a single health expert at a time, which is almost impossible in the physical environment [4], [5], [6]. This paper discusses the recent medical issues -coronavirus in detail with a possible framework capable of predicting the COVID-19 with high accuracy.

The World Health Organization (WHO) got the first update on COVID-19 in December 2019 and then declared a public health emergency in January 2020<sup>1</sup>. Coronavirus is a deadly virus that has

spread over the world and has been a global health hazard since its inception [7], [8], [9], [10]. This virus first infected animals, then humans. If a human comes into contact with an infected animal, it will become infected. The coronavirus is commutable, which means that if one person becomes sick, all those who come into touch with them may also become infected. The coronavirus can spread through respiratory droplets when someone chats with others, sneezes or coughs.

Many health issues are started in human beings infected with the coronavirus. Such as respiratory failure, liver issues, and others [7], [11], [10]. The virus created both short and long-term health issues. When the person is infected, they are being cured with timely treatment. But, if the infected person has some pre-existing disease, then the chances of being cured are very less.

During the first wave of COVID-19, September 2020 received the highest case at 2,622,328 whereas, in the second wave, it increased to 9,016,561 in May 2021. The USA is the most infected country whereas India is present in the second position. Brazil, UK and Russia stand at the 3rd, 4th and 5th positions.

In India, during the peak of the first wave, i.e., in September 2020, 33,424 deaths were reported, whereas, during the second wave, 131,084 death were reported in a single month of May 2021. These statistics indicate their impact on human beings. Every months thousands of lives are lost due to this virus. Even hospitals are full and unable to occupy the infected persons for treatment. During the second wave of the COVID-19, the shortage of Oxygen in various places was also reported<sup>2,3</sup>.

<sup>1</sup> <https://www.who.int/emergencies/diseases/novel-coronavirus-2019?>

\* Corresponding author.

E-mail addresses: [pkroynitp@gmail.com](mailto:pkroynitp@gmail.com) (P. K. Roy),  
[ashish.singhfc@kiit.ac.in](mailto:ashish.singhfc@kiit.ac.in) (A.Singh).

<sup>2</sup> <https://www.dw.com/en/india-covid-oxygen-shortage/a-57425951>, [accessed online: 08-10-2021]

<sup>3</sup> <https://www.bbc.com/news/world-asia-india-57911638>, [accessed online: 08-10-2021]

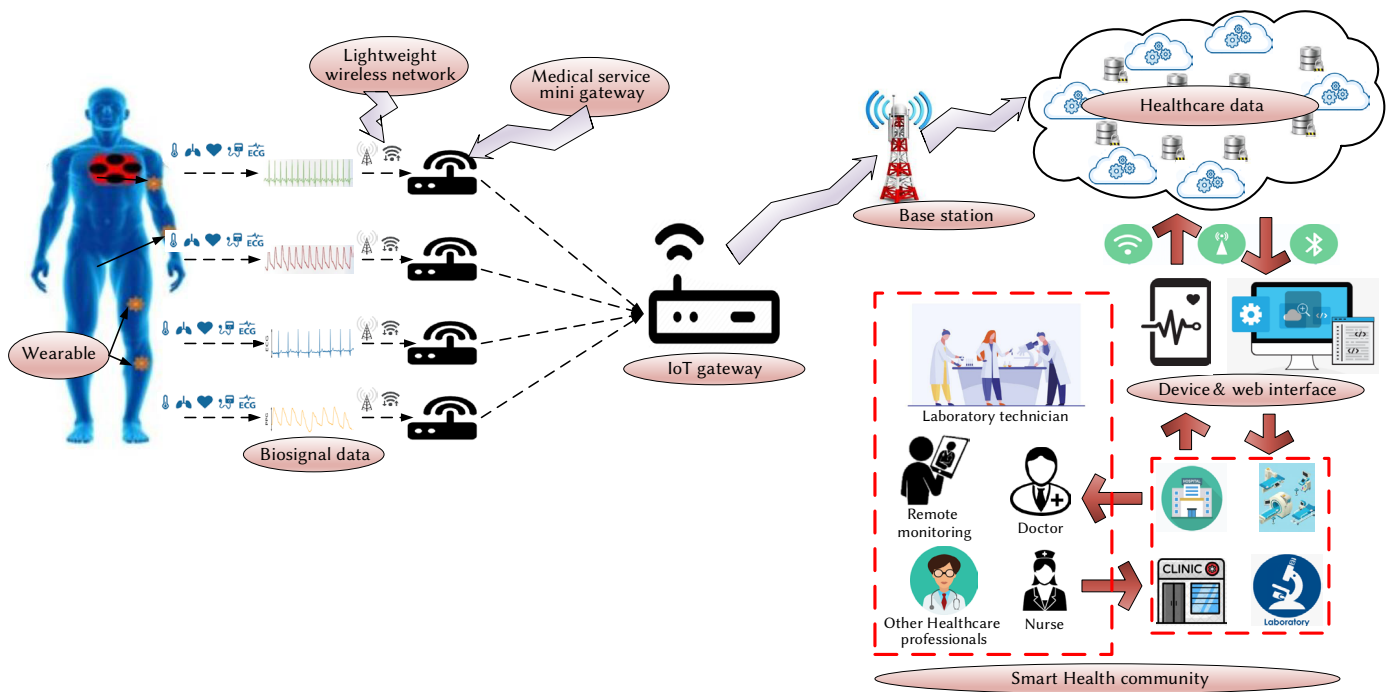


Fig. 1. Framework of Internet of Medical Things Scenario.

Currently, the test name called reverse transcription- polymerase chain reaction (RT-PCR) is used to check whether the person is infected or not from COVID-19. However, RT- PCR test kits take around 4-6 hours to provide the test result [12]. Meanwhile, many people may get infected by each other. The 4-6 hours time to get the result about the infection is an issue to stop it from spreading. The other alternatives that were developed recently include examining CT-scan [9], [13], Chest X-ray [8], [11], [14], reports and other symptoms of suspicious people. Many models reported in the literature have False Positive prediction issues, which means the test result is positive even though people are not infected.

The poor prediction rate and false prediction may have multiple reasons. One reason is less number of actual health reports of the infected person. This research developed a weighted ensemble transfer learning model for COVID-19 detection. The proposed model aims to minimize false-positive prediction cases. The model works in two folds: first, the Chest X-ray images are processed and passed to the pre- trained transfer model. Based on the training performances, the model's weights are decided. Secondly, the outcomes of the three transfer learning models are weighted and ensemble to get the final results. Finally, the developed model can be embedded with an application for real-time COVID-19 predictions. The major contributions of this research include the following:

- A weighted ensemble transfer learning framework is developed in this research for predicting COVID-19 patients.
- The proposed model uses only the Chest X-ray images for training purposes and achieves high accuracy with a minimal false positive prediction rate. The model can be embedded in the portable application for fast COVID-19 prediction.

The rest of the paper is organized as follows: Section II discusses the relevant work related to our objective. In Section III, the model overview is discussed. Section IV discusses a proposed methodology in detail. In Section V, the outcomes of the individual and ensemble learning models are presented, and finally, Section VI concludes this work.

## II. LITERATURE REVIEW

This section discusses existing works for the detection of coronavirus disease. Most recent research uses the benefits of transfer learning models to design the COVID-19 predictive framework [14], [15], [16], [17]. In [18], Chest X-ray radiographs images are used to build the model for coronavirus detection. They have used multiple pre-trained Convolutional Neural Network (CNN) models during the experiment and achieved a 99.70% classification performance using the ResNet50 model. A COVID-19 detection technique has been proposed in [19] using deep learning and transfer learning schemes. They have used X-rays and CT-scan images that are collected from many sources. Their modified CNN model achieved 94.10% accuracy, whereas, with a pre-trained model, 98% accuracy was achieved. A binary and multi-class classification COVID-19 detection mechanism has been proposed in [20]. The experiment was performed on raw Chest X-ray images. Their model achieved the classification accuracy 98.08% for binary classes and 87.02% for multi-class classification of COVID-19 patients.

Another model proposed using the Chest X-ray images for COVID-19 detection in [16]. The authors used an open source dataset for the model development. To develop detection mechanisms, the model uses VGG-16, OxfordNet with Faster Regions CNN. Their model achieved 97.36% accuracy for the best case. In [17], a CoroNet model for detection of COVID- 19 infection has been proposed. Their model was based on Xception architecture and pre-trained on the ImageNet Chest X-ray dataset. In [21], three deep learning-based s were used for the detection and diagnosis of COVID-19 cases. Deep neural network based CNN s are applied to the X-ray images of lungs to diagnose the disease. The results with the CNN model show maximum accuracy of 93.20%. A deep learning technique based on CNN and LSTM has been proposed in [22] for the diagnosis of COVID-19 disease. In this technique, feature extraction was handled by the CNN and detection of the disease is handled by the LSTM model using extracted features. In [8], fine-tuned deep learning techniques have been proposed to speed up the detection and classification of COVID-19 disease. The research was conducted on two different datasets containing 959 X-ray images. DenseNet121 shows higher accuracy, 97% for the first

dataset, and MobileNetV2 has 81% for the second dataset. In [23], authors proposed a diagnosis model for COVID-19 disease. They have used ResNet-50 and DenseNet-201 pre-trained networks for feature extraction and backpropagation neural network model to classify the results into multiple levels. Their model achieved 98.50% accuracy.

In [24], authors proposed an automated technique for COVID-19 detection by using CT-scan images. Their ET-NET model has been evaluated on publicly available data using deep learning techniques. Two different approach used for detection of COVID-19 infection by [25]. Firstly, they used Artificial Neural Networks (ANN) and then Bidirectional Long Short-Term Memories (Bi-LSTM) model was used to design the proposed hybrid architecture. A modified ensemble deep learning models with the inclusion of extra layers has been proposed in [26]. For binary classification model their model achieves 99.49% accuracy and whereas for multi-class, the accuracy value was 99.24%. Machine learning (ML) and transfer learning s based COVID-19 detection model has been proposed in [27]. They have used 5,480 samples having two classes for their experimental purpose. Another work [28], uses a multi-stage transfer learning technique for diagnosis of COVID-19 using CT-scan images with 86.70% accuracy. In [29], Lung CT-scan images are used for COVID-19 infection detection using ensemble classifier. The proposed detection model uses a transfer learning approach with eight different pre-trained models. In [10], authors used an ensemble transfer learning models to build a COVID-19 detection model. They used Chest X-ray images to design the COVID-19 detection framework with pre-trained transfer learning models. The researchers have suggested multiple frameworks to address COVID-19 detection issues and have achieved good accuracy. However, one of the limitations of the existing research includes the dataset used for model development. This research uses a comparatively larger dataset to develop the model. Also used a novel weight assignment approach to build the ensemble framework. The model can be embedded with devices having Internet connectivity. This enables remote monitoring facilities in the healthcare domain and limits the crisis of health experts.

### III. MODEL OVERVIEW

This section mainly highlights the configuration and working of the Transfer Learning (TL) models and ensemble frameworks. First, the working of TL models are explained in detail, and then the reason behind selecting the few TL model will be discussed. At last, the working of the ensemble learning framework and weight generation process are explained in detail.

#### A. Transfer Learning

Along with technological developments, training deep learning neural networks in recent years received many advancements. The main reason behind using the concept of TL is to utilize the existing complex and successful pre-trained models [30] learned from a huge data corpus, viz., (ImageNet model trained with 1000 categorical dataset) and transfer the learnt knowledge [31] to the simple task like binary image classification (COVID-19 Positive, COVID-19 Negative) having less number of data samples. The labelled data can achieve the optimal mapping of images, labels, and sentences. However, the issues of generalizability are still observed when the model is used with unseen and different datasets.

Mathematically, if ImageNet TL has input data ( $I_s$ ), the labels ( $L_s$ ) have 1000 categories, and their corresponding output, i.e., the trained classifier, will be represented using  $O_s$ .

The knowledge of the transfer learning can be represented as in (1).

$$S = \{X_s, L_s, O_s\} \quad (1)$$

Next, the aim is to utilize the source knowledge for building a new model with target input data  $X_t$ , labels  $L_t$  (COVID-19 Positive, COVID-19 Negative), and the model  $O_t$  (see (2)).

$$T = \{X_t, L_t, O_t\} \quad (2)$$

The classifier or model built by utilizing the knowledge of TL can be written as  $O_t(X_t, L_t|S)$ , whereas a model built without using the TL can be written as  $O_t(X_t, L_t)$ . It can be represented as in (3).

$$O_t = \begin{cases} O_t(X_t, L_t|S) & \text{with TL concept} \\ O_t(X_t, L_t) & \text{without TL concept} \end{cases} \quad (3)$$

The model built by utilizing the TL concept, i.e., ( $O_t(X_t, L_t|S)$ ) is probably more suitable for the said problem than the model developed without using the TL concept. This means assuming the large input sample  $X$  has labels  $L$ . The error  $e$  is assumed to be lesser with the TL concept-based model.

$$error[O_t(X_t, L_t|S), (X), L] < error[O_t(X_t, L_t), (X), L] \quad (4)$$

where  $error$  (4) is a function used to calculate the error for input values, the pre-trained model generally helps the user save time, efficiency, and resources as tuning the parameter may not be necessary. The pre-trained models help extract the low-level features from the input images, such as shades and tints. The target model needs only to tune the parameter of the last few last layers.

Instead of directly using the transfer learning models and their weights in the proposed methodology, a weight generation function architecture is used to assign weights to respective models. After referencing several research papers, we found that the transfer learners ResNet50V2, DenseNet201 and InceptionV3 have performed exceptionally well in image classification challenges. Hence, these three individual models have been used and explored for the study.

#### B. Ensemble Learning

The ensemble approach involves combining the predictive power of various learners to improve the overall performance and robustness of the model. The error in the predictive capacity of a model can be decomposed into three errors—bias, variance, and variance of the irreducible error of the model. The model error can be described as Model-Error which is a collective sum of errors obtained from bias, variance, and irreducible error.

The term Bias error is used to describe how much the expected values vary from the actual value on average. A high bias results from under-performance where the model misses important trends during the training phase. Variance indicates the predictive capacity of a model on the same observation. A model tends to overfit with high variance and would perform worse in the validation data set. Various ensemble approaches have been proposed to address this bias-variance trade-off. The optimal scenario is to reach a minimum bias error and a minimum variance error. The reducible error (Bias error and Variance error) is the element that can be improved. We reduce the quantity when the model learns on a training dataset. We attempted to get this quantity as close to zero to reduce the overall error in the model's predictive capacity. The fundamental error is the error that can not be removed. The error is generated because of noise in the observations or outliers in the data set.

The novel contribution to the research is that the different transfer learning architectures were assigned weights depending upon their predictive accuracy over a dataset. The ensemble version is the weighted average of the individual transfer learning-based model's performances obtained with the test dataset.

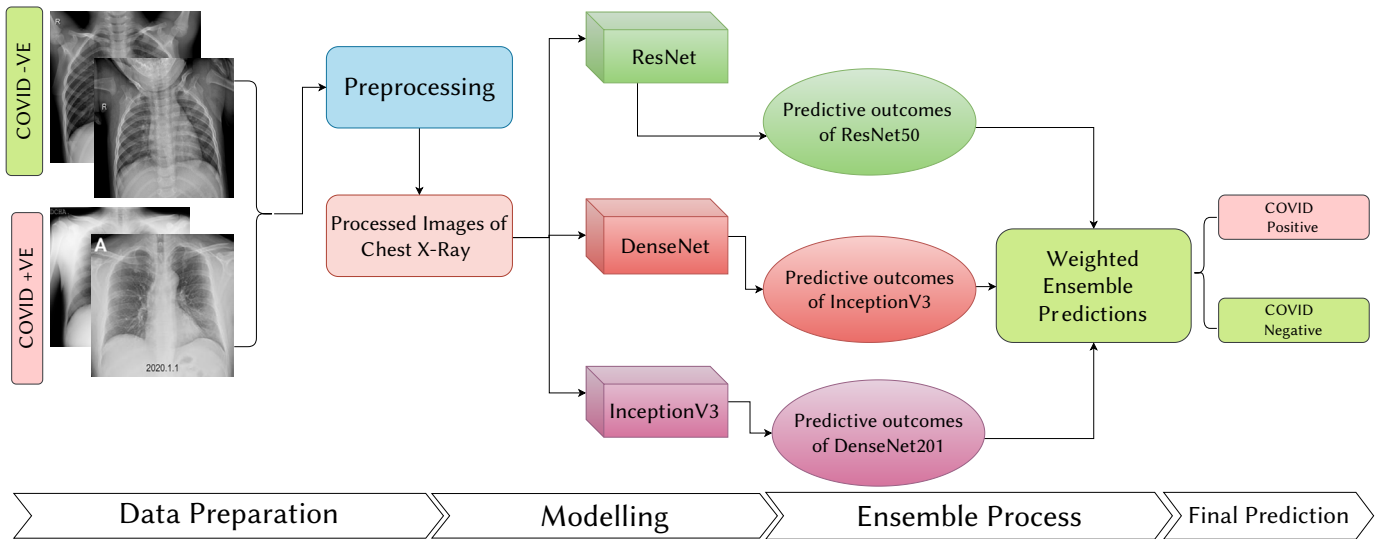


Fig. 2. An overview of the proposed weighed ensemble transfer learning frameworks.

#### IV. PROPOSED METHODOLOGY

The proposed deep ensemble TL framework works two-fold. Firstly, the TL models were to train the data set, i.e., Chest X-ray (CXR) images and generate the corresponding model files. Secondly, to test the real-time inference of the proposed model, 5-Fold cross-validation was used on the validation set, and the corresponding accuracy and loss function graphs were plotted to check the model's performance over increasing epochs on unseen data. Finally, the model files were used to predict the respective Chest X-ray images and their probabilities of belonging to that class. Fig. 2 shows the overview of the working steps involved in the proposed ensemble framework Fig. 3 shows the detailed steps of the proposed models, like the weight generation steps, the data used for the 5-fold cross-validation technique, the metrics used for the evaluation of the model and others.

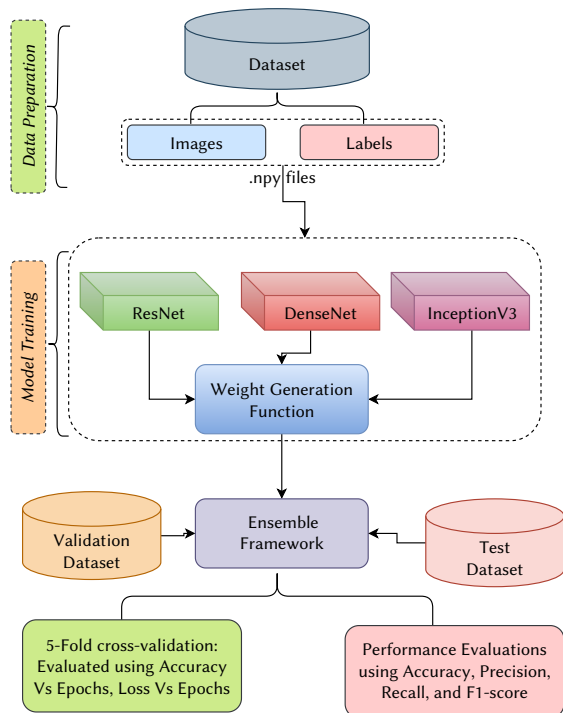


Fig. 3. Detailed steps involved in the proposed weighed ensemble transfer learning framework.

The data set used in this research was collected from <https://www.kaggle.com/tawsifurrahman/covid19-radiography-database>, which has collated images from various sources. Considering the computational resource restraints, a part of the data set was used for the experiment consisting of 2000 images. The model classified the image into two classes (i) "COVID-19 Positive" and (ii) "COVID-19 Negative". A total of 2000 Chest X-ray images were used for the experiment. The detailed break up of the number of images in the data set has been shown in Table I. For optimal model performance, the training and validation sets have been split into 60%, 20%, and 20% ratios, respectively.

TABLE I. DATA DISTRIBUTIONS USED FOR MODEL TRAINING, VALIDATION AND TESTING PURPOSE

| Class             | Train | Test | Validation | Total |
|-------------------|-------|------|------------|-------|
| COVID-19 Positive | 600   | 200  | 200        | 1000  |
| COVID-19 Negative | 600   | 200  | 200        | 1000  |
| Total             | 1200  | 400  | 400        | 2000  |

The images correspond to the "COVID-19 Positive" class, and the "COVID-19 Negative" class was converted to ".npy" files and their appropriate labels. The ".npy" file format is NumPy's basic binary file format for storing a single NumPy array on a disk. This way, the shape and the data type information necessary to create the array on a system with different architecture remains intact. This process leads to faster processing of data. All of the images from the source were 299x299 pixels in nature, which had been converted to an appropriate size of 224x224 pixels to suit the respective transfer learning architecture. The code structure appends the data and the images according to their respective classes and labels and stores it in a standard binary format, the ".npy" file. Threading was used for the parallel execution and utilized the multiprocessing capacity to optimal. 1 discusses the complete working steps of data preparation.

##### A. Model Training

Three pre-trained TL models, (i) ResNet50V2, (ii) DenseNet201 and (iii) InceptionV3, were used during the training phase proposed model. The models were trained with 200 epochs, and the learning rate was fixed to 0.001, with a batch size of 32. The callback function was explicitly used to monitor the model performance by fixing the patience value of 5. This means, the model will stop training for further epochs if they encounter no improvement in the validation accuracy in five consecutive epochs. The model was compiled using

TABLE II. DETAILS OF THE PARAMETERS USED FOR MODEL DEVELOPMENT WITH RESNET50V2, DENSENET201, AND INCEPTIONV3

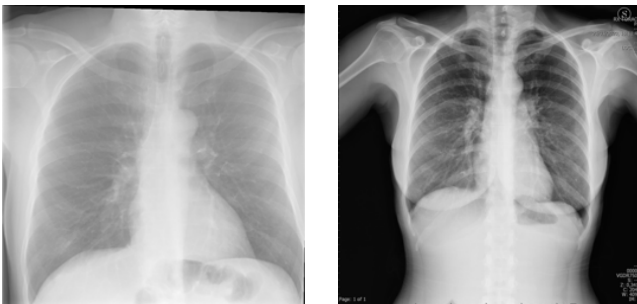
| Parameters                | ResNet50V2                       | DenseNet201                      | InceptionV3                      |
|---------------------------|----------------------------------|----------------------------------|----------------------------------|
| Learning Rate             | 0.001                            | 0.001                            | 0.001                            |
| Batch Size                | 32                               | 32                               | 32                               |
| Number of epochs trained  | 20                               | 35                               | 19                               |
| Loss Function             | Sparse Categorical Cross Entropy | Sparse Categorical Cross Entropy | Sparse Categorical Cross Entropy |
| Training Time             | 287 seconds                      | 987 seconds                      | 310 seconds                      |
| Accuracy on Test Data set | 98.75%                           | 99.75%                           | 98.25%                           |
| Weights assigned          | 0.75235685                       | 0.76147539                       | 0.7513245                        |

**Algorithm 1.** Data preparation for model training

```

1: Input: Raw Images
2: Output: .npy files
3: BEGIN
4: create data()
5: data = [ ]
6: for category in categories do
7:   a. path = location of the files
8:   b. class num = categories.index(category)
9:   c. files = loaded from path
10:  d. total = number of files
11:  e current = 1
12:  for img in files: do
13:    1. try:
14:      a. img array = read image from path
15:      b. img array = resize the image
16:      c. data.append([img array,class num])
17:    2. except Exception as e:
18:      a. pass
19:    3. current += 1
20: random.shuffle(data)
21: images = [ ] 22: classes = [ ] 23: current = 1
24: for image, cls in data: do
25:   a. images.append(image)
26:   b. classes.append(cls)
27:   c. current += 1
28: images = np.array(images).reshape(-1,image size, im- age size,3)
29: images = images/255.0
30: classes = np.array(classes) #Preparing .npy files
31: np.save(save filename images,images)
32: np.save(save filename labels,classes)
33: END

```



(a) COVID- 19 Positive (b) COVID- 19 Positive

Fig. 4. Chest X-ray of COVID-19 Positive patient.

Adam Optimizer, with the exponential decay rate for the first moment being 0.90 and for the second moment being 0.999. The ensemble function calculates the weighted average of predicted models based on their weights, respectively. The individual weights were assigned based on predictive accuracy. A sigmoid function was applied to it to give the probability of occurrence.

The performance of the trained model on an unseen dataset was evaluated using the performance metrics like F1-score, Precision and Recall. The values of these metrics are calculated using the parameter of the confusion metrics, such as true positive (TP), false positive (FP), true negative (TN), and false-negative (FN). Mathematically, these metrics are defined in Eqs. (5)-(8):

$$Precision = \frac{TP}{TP + FP} \quad (5)$$

$$Recall = \frac{TP}{TP + FN} \quad (6)$$

$$F1 - score = \frac{Precision * Recall}{Precision + Recall} \quad (7)$$

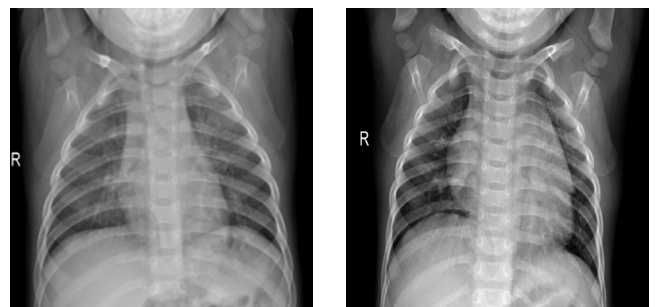
$$Accuracy = \frac{TP + TN}{TP + TN + FP + FN} \quad (8)$$

## V. RESULTS

This section discusses the experimental outcomes of the proposed deep ensemble TL models in different hyper-parameter settings. As discussed, a weight generation function was used to generate the weight of the individual TL models based on their prediction accuracy. The weights are generated using the sigmoid function, resulting in the class probabilities in [0-1]. Table III consists of the name of the models, the time taken for training, the accuracy obtained on the test dataset and the weights generated by the weight generation function.

TABLE III. INDIVIDUAL MODEL'S ACCURACY AND CORRESPONDING WEIGHTS DEFINED BY WEIGHT GENERATION FUNCTION

| Parameters                | ResNet50V2  | DenseNet201 | InceptionV3 |
|---------------------------|-------------|-------------|-------------|
| Training Time             | 279 seconds | 899 seconds | 260 seconds |
| Accuracy on Test Data set | 98.75%      | 99.75%      | 98.25%      |
| Weights assigned          | 0.75235685  | 0.76147539  | 0.7513245   |

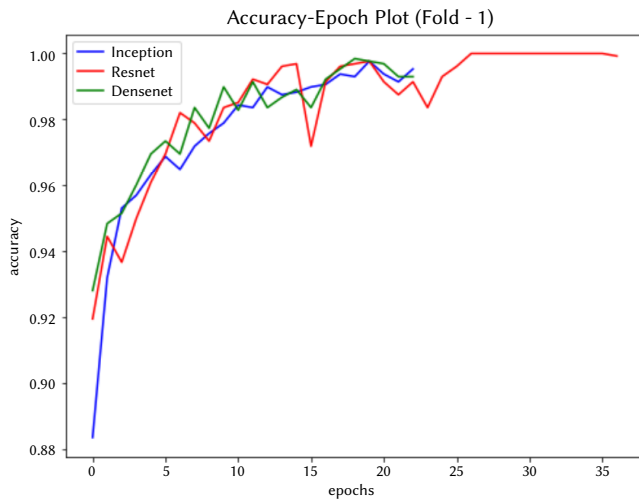


(a) COVID- 19 Negative (b) COVID- 19 Negative

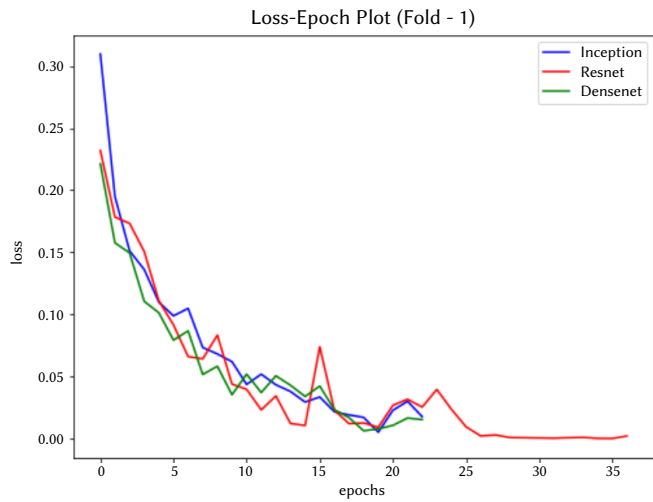
Fig. 5. Chest X-rays of COVID-19 Negative patient.

TABLE IV. THE PERFORMANCE OBTAINED WITH RESNET50V2, DENSENET201, AND INCEPTIONV3 IN DIFFERENT K-FOLDS

| Fold No.                      | Fold 1      |             |             | Fold2       |             |             | Fold 3      |             |             |
|-------------------------------|-------------|-------------|-------------|-------------|-------------|-------------|-------------|-------------|-------------|
|                               | ResNet50V2  | DenseNet201 | InceptionV3 | ResNet50V2  | DenseNet201 | InceptionV3 | ResNet50V2  | DenseNet201 | InceptionV3 |
| Parameters                    |             |             |             |             |             |             |             |             |             |
| No of epochs actually trained | 37          | 23          | 23          | 37          | 30          | 34          | 19          | 29          | 25          |
| Train Time                    | 301         | 365         | 221         | 301 seconds | 435 seconds | 279 seconds | 157 seconds | 454 seconds | 208 seconds |
| Accuracy on validation set    | 96.25%      | 93.25%      | 97.50%      | 98.00%      | 97.50%      | 96.25%      | 84.00%      | 98.25%      | 95.25%      |
| Weights assigned              | 0.72237036  | 0.72237036  | 0.72487028  | 0.72424661  | 0.72487028  | 0.72611498  | 0.7051357   | 0.72048628  | 0.72237036  |
| Ensemble Model's Accuracy     | 97.25%      |             |             | 97.75%      |             |             | 97.00%      |             |             |
| Fold No.                      | Fold 4      |             |             | Fold 5      |             |             |             |             |             |
|                               | ResNet50V2  | DenseNet201 | InceptionV3 | ResNet50V2  | DenseNet201 | InceptionV3 |             |             |             |
| Model                         |             |             |             |             |             |             |             |             |             |
| No of epochs actually trained | 27          | 28          | 19          | 29          | 31          | 37          |             |             |             |
| Train Time                    | 221 seconds | 439 seconds | 159 seconds | 238 seconds | 485 seconds | 303 seconds |             |             |             |
| Accuracy on validation set    | 97.75%      | 96.50%      | 96.25%      | 97.75%      | 97.25%      | 97%         |             |             |             |
| Weights assigned              | 0.72174321  | 0.72237036  | 0.72299665  | 0.73044372  | 0.73044372  | 0.72921135  |             |             |             |
| Ensemble Model's Accuracy     | 98.00%      |             |             | 97.75%      |             |             |             |             |             |

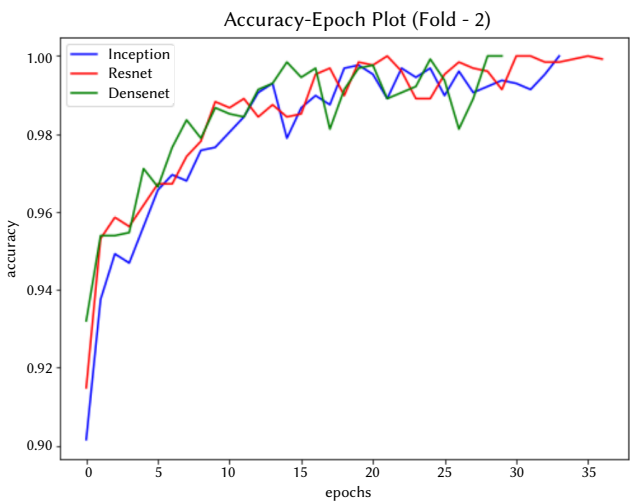


(a) Accuracy vs Epochs

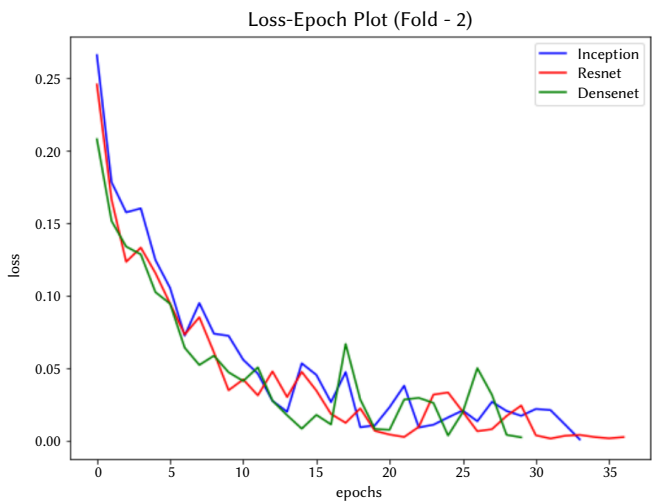


(b) Loss vs Epochs

Fig. 6. The plot of accuracy and losses obtained with different epochs for Fold 1 of the cross-validation technique.



(a) Accuracy vs Epochs



(b) Loss vs Epochs

Fig. 7. The plot of accuracy and losses obtained with different epochs for Fold 2 of the cross-validation technique.

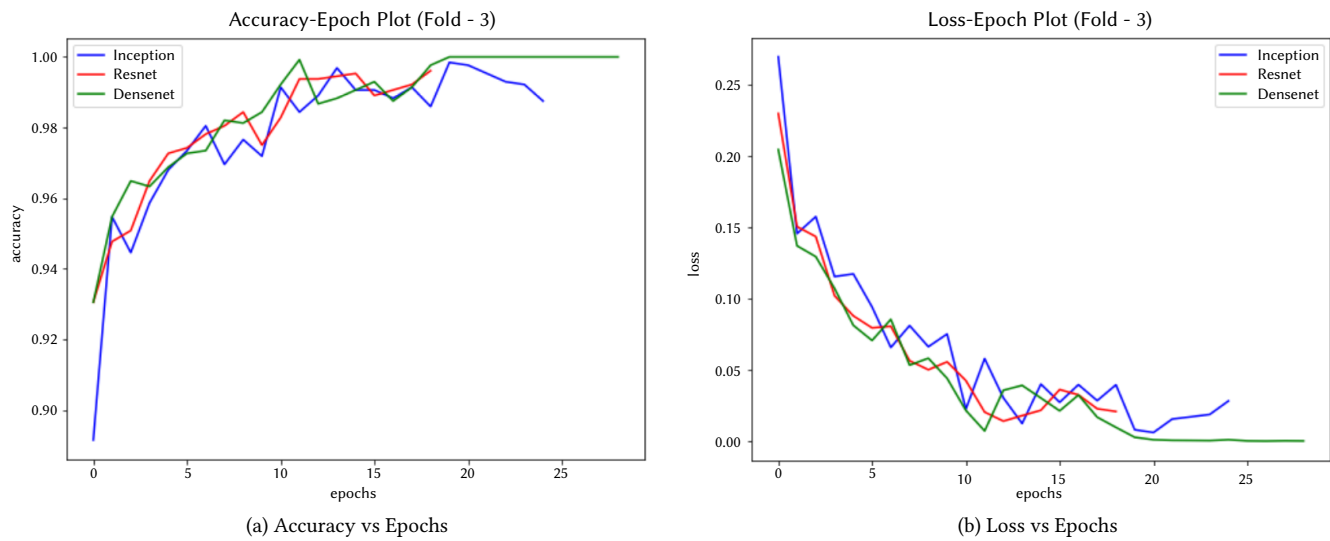


Fig. 8. The plot of accuracy and losses obtained with different epochs for Fold 3 of the cross-validation technique.

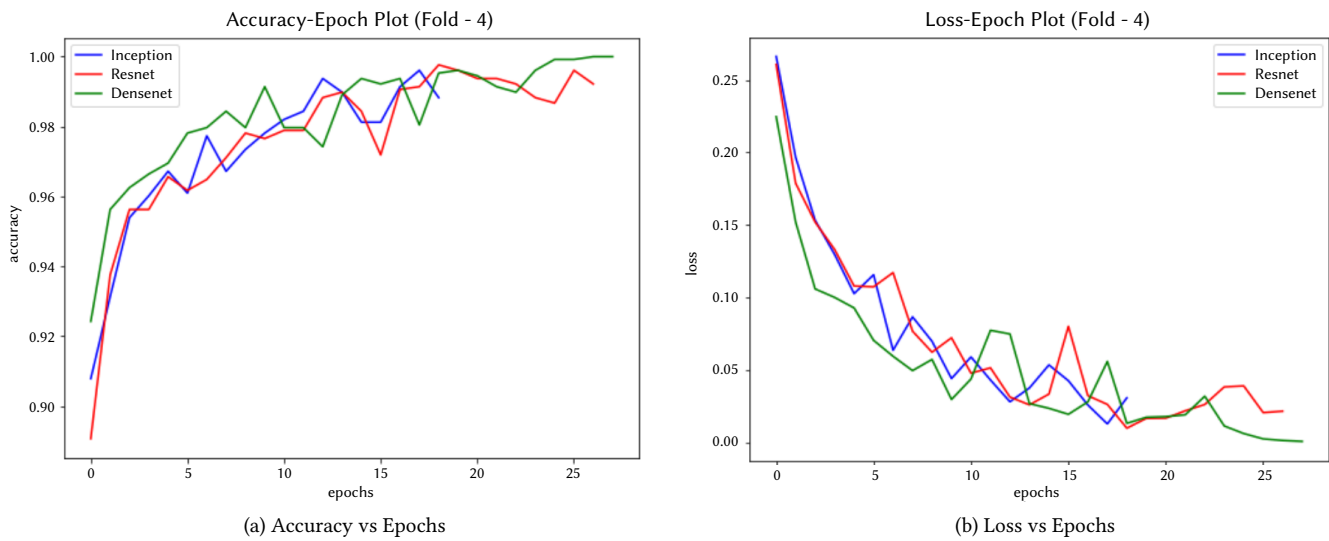


Fig. 9. The plot of accuracy and losses obtained with different epochs for Fold 4 of the cross-validation technique.

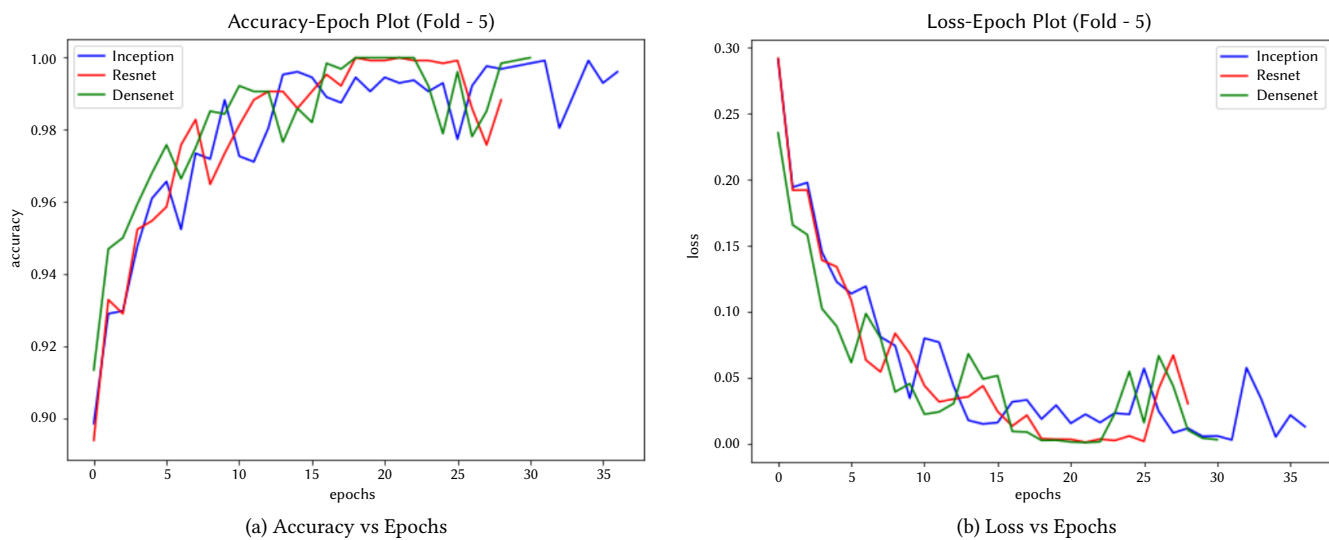


Fig. 10. The plot of accuracy and losses obtained with different epochs for Fold 5 of the cross-validation technique.

TABLE V. PERFORMANCE OF PROPOSED ENSEMBLE MODEL ON MANUALLY WEIGHTED AND WEIGHTED WITH A FUNCTION

| Models                   | DenseNet   | ResNet     | InceptionV3 | TP  | TN  | FP | FN | Precision | Recall | F1           |
|--------------------------|------------|------------|-------------|-----|-----|----|----|-----------|--------|--------------|
| Manual Weight Assignment | 0.10       | 0.60       | 0.30        | 200 | 196 | 0  | 4  | 0.990     | 0.980  | 0.990        |
|                          | 0.50       | 0.20       | 0.30        | 200 | 195 | 0  | 5  | 0.995     | 0.990  | 0.995        |
|                          | 0.10       | 0.80       | 0.10        | 200 | 195 | 0  | 5  | 0.987     | 0.976  | 0.987        |
|                          | 0.10       | 0.10       | 0.80        | 200 | 194 | 0  | 6  | 0.985     | 0.970  | 0.985        |
| Weighted by function     | 0.75235685 | 0.76147539 | 0.7513245   | 200 | 197 | 0  | 3  | 0.997     | 0.995  | <b>0.997</b> |

TABLE VI. PERFORMANCE COMPARISON WITH EXISTING RESEARCH

| Models                  | Number of samples | Types of data | Technique                         | Precision    | Recall       | F1-score     |
|-------------------------|-------------------|---------------|-----------------------------------|--------------|--------------|--------------|
| Islam et al. [22]       | 1525              | CXR           | CNN, LSTM                         | –            | 0.993        | 0.989        |
| Khan et al. [17]        | 284               | CXR           | DCNN                              | 0.93         | 0.982        | –            |
| Ozturk et al. [20]      | 127               | CXR           | DCNN                              | 0.98         | 0.951        | 0.965        |
| Shibly et al. [16]      | 283               | CXR           | RCNN                              | 0.9929       | 0.976        | 0.984        |
| Hassantabar et al. [21] | 200               | CT            | CNN and DNN                       | –            | 0.960        | –            |
| Maghdid et al. [19]     | 431               | CT and CXR    | CNN and Transfer Learning         | –            | 0.960        | –            |
| <b>Proposed</b>         | <b>2000</b>       | <b>CXR</b>    | <b>Ensemble Transfer Learning</b> | <b>0.997</b> | <b>0.995</b> | <b>0.997</b> |

### A. Performance With K-Fold Setting

To check the model's performance on unseen data using the K-fold setting. The experiment was repeated with the same set of TL models. The value of K was fixed to 5. In K-Fold cross-validation, the data is split into K folds. K-1 folds act as a training set for each iteration, whereas the remaining fold is a test set. This results in less bias and better performance because each observation in the original data set is optimally used.

The performance of the K-fold cross-validation technique was checked over an increasing number of epochs. The hyper-parameters values remain the same as the previous setting as discussed in section IV-A. In the proposed model, each transfer learner was individually trained for all the 5-Folds, and a corresponding ensemble accuracy was calculated for each fold. Table IV shows the experimental outcomes of K-fold settings with the value of the used parameter. The accuracy value obtained on different K-folds, i.e., Fold 1, Fold 2, Fold 3, Fold 4, and Fold 5, are 97.50%, 97.75%, 97.00%, 98.00%, and 97.75%, respectively. The accuracy value for the different K-fold settings lies between 97.00% to 98.00%. For each fold, *Accuracy vs Epoch*, and *Loss vs Epoch* graphs are plotted to check how the model performs on the validation data (unseen). The plots are shown in Fig. 6 to Fig. 10.

### B. Performance Comparison With Manual Weight Assignments

As shown in Table V, the performance of the proposed weighted ensemble TL framework achieved satisfactory performance. To verify the weights generated by the function, we have manually assigned the weights to the individual TL models as shown in Table V and checked their performances. In the first case, the weight of DenseNet, ResNet, and InceptionV3 was 0.10, 0.60, 0.30. The model yielded precision, recall, and F1-score value of 0.990, 0.980, and 0.990, respectively. In the second case, the weight of DenseNet, ResNet, and InceptionV3 was 0.50, 0.20, 0.30. The model yielded precision, recall, and F1-score values of 0.995, 0.990, and 0.995. In the third case, the weight of DenseNet, ResNet, and InceptionV3 was 0.10, 0.80, 0.10. The model yielded precision, recall, and F1-score values of 0.987, 0.976, and 0.987. In the fourth case, the weight of DenseNet, ResNet, and InceptionV3 was 0.10, 0.10, 0.80. The model yielded precision, recall, and F1-score values of 0.985, 0.970, and 0.99.

Finally, the model's performance with the manual weight assignment technique was compared with the performance obtained using automated weight assignment techniques, where the precision, recall, and F1-score were 0.997, 0.995, and 0.997, respectively. The proposed automated weight assignment technique helps achieve

better performance. The confusion matrix's parameter values were as follows: the true positive (TP) is 197, FP is 0, TN is 197, and FN is 3, indicating that the model misclassifies only three samples among the total test sample. The confusion matrix obtained using the best model setting is shown in Fig. 11.

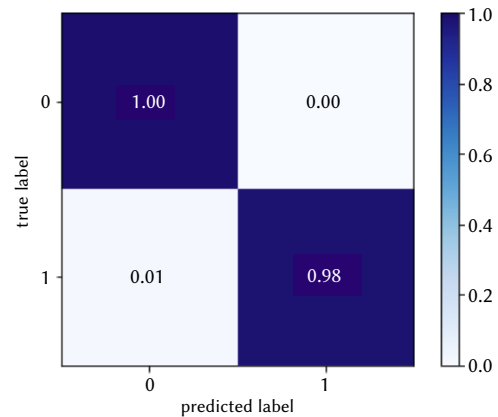


Fig. 11. Confusion matrix obtained using the best model.

### C. Performance Comparison With State-Of-The-Art

The experimental outcomes of the proposed weighted ensemble TL model were compared with the existing deep learning-based COVID-19 predictive models in Table VI. It can be seen that the proposed weighted ensemble TL models outperformed existing research. As compared to the listed research (Islam et al. [22], Khan et al. [17], Ozturk et al. [20], Shibly et al. [16], Hassantabar et al. [21], Maghdid et al. [19]), this research consider more number of data CXR samples to train and validate the model. Among the existing researchers, Islam et al. [22] achieved the best prediction performance, where the recall value was 0.993 and F1-score was 0.989. However, the proposed model achieved the F1-score of 0.997, outperforming the existing research.

## VI. CONCLUSION

The healthcare industry is equipped with the latest technologies to provide the best treatment for patients suffering from critical diseases. Recent technology like the Internet of Things (IoT) can also be used for various purposes in the medical field, like remote monitoring of patient health. This study suggested an Internet of



Medical Things-assisted framework to fulfil medical experts' needs during the COVID-19 pandemic. The proposed framework uses the weighted average of predictive accuracy of individual transfer learning models, namely ResNet50V2, DenseNet201 and InceptionNetV3. The ensemble learning framework uses the individual strength of the transfer learners to detect COVID-19 from the Chest X-ray images. The model performs well on the validation data set, which can be observed from the results of the 5-Fold cross-validation. The IoMT based model helps predict and monitor COVID-19 patients remotely with the embedded application. The proposed model's performance can be improved by using the Regularization techniques such as Data Augmentation and Generative Adversarial Networks. Despite its heavy computational requirements and complex structure, this framework is practical enough to provide optimal results on the validation data set. The dataset used in this research can be extended using some preprocessing techniques. The model works on the posterior-anterior (PA) view of X-Rays. Hence it can not differentiate anterior-posterior (AP), lateral views etc. The problem can be further extended to predict the mild and severe cases of COVID-19. This would reduce the load on the existing healthcare infrastructure. Also, there is a need for efficient radiologists to identify and confirm the results of the proposed model.

#### DECLARATION OF COMPETING INTEREST

There is no Conflict of Interest.

#### REFERENCES

- [1] P. Verma and S. K. Sood, "Fog assisted-iot enabled patient health monitoring in smart homes," *IEEE Internet of Things Journal*, vol. 5, no. 3, pp. 1789–1796, 2018.
- [2] M. Kang, E. Park, B. H. Cho, and K.-S. Lee, "Recent patient health monitoring platforms incorporating internet of things-enabled smart devices," *International neurology journal*, vol. 22, no. Suppl 2, p. S76, 2018.
- [3] O. Taiwo and A. E. Ezugwu, "Smart healthcare support for remote patient monitoring during covid-19 quarantine," *Informatics in medicine unlocked*, vol. 20, p. 100428, 2020.
- [4] D. V. Dimitrov, "Medical internet of things and big data in healthcare," *Healthcare informatics research*, vol. 22, no. 3, pp. 156–163, 2016.
- [5] W. Sun, Z. Cai, Y. Li, F. Liu, S. Fang, and G. Wang, "Security and privacy in the medical internet of things: a review," *Security and Communication Networks*, vol. 2018, 2018.
- [6] F. Hu, D. Xie, and S. Shen, "On the application of the internet of things in the field of medical and health care," in *2013 IEEE international conference on green computing and communications and IEEE Internet of Things and IEEE cyber, physical and social computing*. IEEE, 2013, pp. 2053–2058.
- [7] S. Chahar and P. K. Roy, "Covid-19: A comprehensive review of learning models," *Archives of Computational Methods in Engineering*, vol. 29, p. 1915–1940, 2021.
- [8] S. Aggarwal, S. Gupta, A. Alhudhaif, D. Koundal, R. Gupta, and K. Polat, "Automated covid-19 detection in chest x-ray images using fine-tuned deep learning architectures," *Expert Systems*, p. e12749.
- [9] S. Shambhu, D. Koundal, P. Das, and C. Sharma, "Binary classification of covid-19 ct images using cnn: Covid diagnosis using ct," *International Journal of E-Health and Medical Communications (IJEHMC)*, vol. 13, no. 2, pp. 1–13, 2021.
- [10] P. K. Roy and A. Kumar, "Early prediction of covid-19 using ensemble of transfer learning," *Computers and Electrical Engineering*, vol. 101, p. 108018, 2022.
- [11] S. Tabik, A. Gómez-Ríos, J. L. Martín-Rodríguez, I. Sevillano-García, M. Rey-Area, D. Chartre, E. Guirado, J. L. Suárez, J. Luengo, M. A. Valero-González, P. García-Villanova, E. Olmedo-Sánchez, and F. Herrera, "Covidgr dataset and covid-sdnet methodology for predicting covid-19 based on chest x-ray images," *IEEE Journal of Biomedical and Health Informatics*, vol. 24, no. 12, pp. 3595–3605, 2020.
- [12] A. Bernheim, X. Mei, M. Huang, Y. Yang, Z. A. Fayad, N. Zhang, K. Diao, B. Lin, X. Zhu, K. Li *et al.*, "Chest ct findings in coronavirus disease-19 (covid-19): relationship to duration of infection," *Radiology*, p. 200463, 2020.
- [13] A. Hiremath, K. Bera, L. Yuan, P. Vaidya, M. Alilou, J. Furin, K. Armitage, R. Gilkeson, M. Ji, P. Fu, A. Gupta, C. Lu, and A. Madabhushi, "Integrated clinical and ct based artificial intelligence nomogram for predicting severity and need for ventilator support in covid-19 patients: A multi-site study," *IEEE Journal of Biomedical and Health Informatics*, vol. 25, no. 11, pp. 4110–4118, 2021.
- [14] V. Dwivedy, H. D. Shukla, and P. K. Roy, "Lmnet: Lightweight multi-scale convolutional neural network architecture for covid-19 detection in iomt environment," *Computers and Electrical Engineering*, vol. 103, p. 108325, 2022.
- [15] A. Kumar, P. K. Roy, and J. P. Singh, "Bidirectional encoder representations from transformers for the covid-19 vaccine stance classification," in *Working Notes of FIRE-13th Forum for Information Retrieval Evaluation, FIRE-WN 2021*, 2021, pp. 1216–1220.
- [16] K. H. Shibly, S. K. Dey, M. T.-U. Islam, and M. M. Rahman, "Covid faster r-cnn: A novel framework to diagnose novel coronavirus disease (covid-19) in x-ray images," *Informatics in Medicine Unlocked*, vol. 20, p. 100405, 2020.
- [17] A. I. Khan, J. L. Shah, and M. M. Bhat, "Coronet: A deep neural network for detection and diagnosis of covid-19 from chest x-ray images," *Computer Methods and Programs in Biomedicine*, vol. 196, p. 105581, 2020.
- [18] A. Narin, C. Kaya, and Z. Pamuk, "Automatic detection of coronavirus disease (covid-19) using x-ray images and deep convolutional neural networks," *Pattern Analysis and Applications*, pp. 1–14, 2021.
- [19] H. S. Maghdid, A. T. Asaad, K. Z. Ghafoor, A. S. Sadiq, S. Mirjalili, and M. K. Khan, "Diagnosing covid-19 pneumonia from x-ray and ct images using deep learning and transfer learning s," in *Multimodal Image Exploitation and Learning 2021*, vol. 11734. International Society for Optics and Photonics, 2021, p. 117340E.
- [20] T. Ozturk, M. Talo, E. A. Yildirim, U. B. Baloglu, O. Yildirim, and U. R. Acharya, "Automated detection of covid-19 cases using deep neural networks with x-ray images," *Computers in biology and medicine*, vol. 121, p. 103792, 2020.
- [21] S. Hassantabar, M. Ahmadi, and A. Sharifi, "Diagnosis and detection of infected tissue of covid-19 patients based on lung x-ray image using convolutional neural network approaches," *Chaos, Solitons & Fractals*, vol. 140, p. 110170, 2020.
- [22] M. Z. Islam, M. M. Islam, and A. Asraf, "A combined deep cnn-lstm network for the detection of novel coronavirus (covid-19) using x-ray images," *Informatics in medicine unlocked*, vol. 20, p. 100412, 2020.
- [23] A. Aswathy, A. Hareendran, and V. C. SS, "Covid-19 diagnosis and severity detection from ct-images using transfer learning and back propagation neural network," *Journal of Infection and Public Health*, vol. 14, no. 10, pp. 1435–1445, 2021.
- [24] R. Kundu, P. K. Singh, M. Ferrara, A. Ahmadian, and R. Sarkar, "Et-net: an ensemble of transfer learning models for prediction of covid-19 infection through chest ct-scan images," *Multimedia Tools and Applications*, vol. 81, no. 1, pp. 31–50, 2022.
- [25] M. F. Aslan, M. F. Unlersen, K. Sabanci, and A. Durdu, "Cnn-based transfer learning-bilstm network: A novel approach for covid-19 infection detection," *Applied Soft Computing*, vol. 98, p. 106912, 2021.
- [26] F. Altaf, S. Islam, and N. K. Janjua, "A novel augmented deep transfer learning for classification of covid-19 and other thoracic diseases from x-rays," *Neural Computing and Applications*, vol. 33, no. 20, pp. 14 037–14 048, 2021.
- [27] S. M. Rezaei, M. Ghorvei, R. Abedi-Firouzjah, H. Mojtahedi, and H. E. Zarch, "Detecting covid-19 in chest images based on deep transfer learning and machine learning s," *Egyptian Journal of Radiology and Nuclear Medicine*, vol. 52, no. 1, pp. 1–12, 2021.
- [28] J. F. H. Santa Cruz, "An ensemble approach for multi-stage transfer learning models for covid-19 detection from chest ct scans," *Intelligence-Based Medicine*, vol. 5, p. 100027, 2021.
- [29] N. S. Shaik and T. K. Cherukuri, "Transfer learning based novel ensemble classifier for covid-19 detection from chest ct-scans," *Computers in Biology and Medicine*, vol. 141, p. 105127, 2022.
- [30] R. Glatt, F. L. Da Silva, R. A. da Costa Bianchi, and A. H. R. Costa, "Decaf: deep case-based policy inference for knowledge transfer in reinforcement learning," *Expert Systems with Applications*, vol. 156, p. 113420, 2020.

- [31] Z. Benbahria, I. Sebari, H. Hajji, and M. F. Smiej, "Intelligent mapping of irrigated areas from landsat 8 images using transfer learning," *International Journal of Engineering and Geosciences*, vol. 6, no. 1, pp. 40–50, 2021.



**Dr Pradeep Kumar Roy**

Dr Pradeep Kumar Roy received his M. Tech and PhD degrees in Computer Science and Engineering from the National Institute of Technology Patna in 2015 and 2018, respectively. He received a Certificate of Excellence for securing a top rank in the M. Tech course. He has been featured in the Top 2% of Scientists in the World list prepared by Stanford University, USA, in 2022. He is currently working as an Assistant Professor at the Department of Computer Science and Engineering, Indian Institute of Information Technology (IIIT) Surat, Gujarat, India. He also worked at Vellore Institute of Technology, Vellore, Tamil Nadu, India. His specialization straddles question answering, text mining and information retrieval, social network, and wireless sensor networks. He has published articles in different journals, including IEEE Transactions on Artificial Intelligence, IEEE Transactions on Network Science and Engineering, Neural Processing Letters, Computers and Electrical Engineering, IJIM, Neural Computing and Applications, Future Generation Computer Systems, Journal of Information Sciences, and others. He has also published conference articles at various international conferences, including ACL, FIRE, IEEE, Springer, and others.



**Dr Ashish Singh**

Dr Ashish Singh is currently working as an Assistant Professor, School of Computer Engineering, Kalinga Institute of Industrial Technology, Deemed to be University, Bhubaneswar, Odisha-751024. He completed his BE and M.Tech in Computer Science and Engineering in 2013 and 2015, respectively. The Ph. D. degree has been received in Computer Science & Engineering from the National Institute of Technology Patna (Bihar), under Visvesvaraya Ph.D. Scheme for Electronics & IT Ministry of Electronics & Information Technology (MeitY) Government of India in 2020. His research areas are cloud security, trust management, healthcare security, Internet of Things, access control, Edge computing, and network security. He has published articles in different Journals, including Journal of Network and Computer Applications, ICT Express, Journal of Ambient Intelligence and Humanized Computing, Multimedia Tools and Applications, Computers and Electrical Engineering, Cluster Computing, IEEE Transactions on Industrial Informatics, IEEE Transactions on Network Science and Engineering, and others. He has also published many conference proceedings at prestigious international conferences. In a special section, he manages the editorial ship as a lead guest editor in Computers and Electrical Engineering and IEEE Transactions on Industrial Informatics Journal.